ORIGINAL PAPER

X-RAY DIFFRACTION AND NANOINDENTATION CHARACTERIZATION OF BONE TISSUE AFFECTED BY SEVERE OSTEOARTHRITIS

CRISTINA MIHAELA NICOLESCU[1], MARIUS BUMBAC[2]*, SIMONA MIHAI[1], ANCA IRINA GHEBOIANU[1], MIHAI CONSTANTIN BALASA[3,4], VIVIANA FILIP[3], STEFAN CUCULICI[5], STEFAN CRISTEA[5], COSMIN PANTU[5]

Manuscript received: 09.01.2018; Accepted paper: 02.03.2018;
Published online: 30.03.2018.

Abstract. *Bone tissue sampled from a patient suffering from osteoarthritis was characterized using X-ray diffraction and nanoindentation. Structural and chemical analysis of bone and cartilage samples showed their crystalline and/or amorphous character, and presence of crystalline phases such as hydroxyapatite $Ca_5(PO4)_3(OH)$, monetite $CaHPO_4$ and brushite $CaPO_3(OH)\cdot 2H_2O$ in various proportions was found. Nanometric crystallite sizes in the range of 1.68 to 17.61 nm were found in the crystalline phases identified in studied bones. Measurements of microhardness (2 MPa) and Young modulus (21 MPa) on cartilage samples along with the anatomical axis of the tibia showed one order differences compared to parameters of cartilage samples measured perpendicular to the long axis of the tibia (57 MPa for microhardness and 368 MPa for Young modulus). Correlations of measured parameters with orthopedic pathology were suggested.*

Keywords: *X-ray diffraction, nanoindentation, bone tissue, orthopedy, osteoarthritis*

1. INTRODUCTION

Bone formation, as well as its composition and structure are subjects of constant interest for medical research field, considering the implants needed for patients with certain diseases. Bones are structured composite materials containing various chemical compounds. The solid constituents are crystalline and/or amorphous, either organic, mineral, and organic-inorganic composites. Bone strength and macro-appearance are influenced by its structure and composition [1].

Knowledge on the mechanical bone tissue properties is of important scientific interest as it may help medical doctors to decide on the appropriate implant, where the case. Once the natural articulation exceeds a certain level of deficiency, its functional role in the patient organism is blocked, so an orthopedic implant replacement may be recommended. Mechanical tests on a wide variety of biomaterials were reported in the last years. Determination of hardness and stiffness were of specific interest for the orthopedic implant choice, and respectively for the fixation on the host-bone system [2].

[1] Valahia University of Targoviste, Institute of Multidisciplinary Research for Science and Technology, 130004 Targoviste, Romania.
[2] Valahia University of Targoviste, Faculty of Science and Arts, Department of Science and Advanced Technologies, 130004 Targoviste, Romania. E-mail: mariusbumbac@gmail.com.
[3] Valahia University of Targoviste, Doctoral School of Engineering Sciences, 130105 Targoviste, Romania.
[4] Macartney Hydraulics A/S, DK-7620 Lemvig, Denmark.
[5] University of Medicine and Pharmacy "Carol Davila", 030167 Bucharest, Romania.

The study is a result of cooperation between Carol Davila University of Medicine and Pharmacy and Valahia University of Targoviste, corresponding activities were carried out in their research facilities, in compliance with all the applicable professional ethics. Bone samples were taken from a patient suffering from the severe osteoarthritis of the knee, secondary to a tibial plateau malunited fracture. Patient had a *Genu varum* deformity with subchondral bone condensation.

The aim of the present work was to explore the usefulness of two analytical techniques for collecting and providing information of medical importance for patients affected by orthopedic pathology, specifically by osteoarthritis.

X-ray diffraction usually gives information related to structure and chemical analysis, qualitative and quantitative, for the crystalline phases that may be present in various samples. Applications related to crystallite dimensions, and presence of nanoparticles could be indicated by the use of this technique [3-6]. Also, XRD may be used for structural characterization of films deposited on different supports [7-9], as may be the case of biocompatible metallic orthopedic implants.

Nanoindentation, together with other mechanical tests, are usually applied for characterization of various solid materials, providing information about their hardness, stiffness, thus on their deformability in specific *in situ* conditions [10-13].

Present study indicated that X-ray diffraction and nanoindentation techniques may provide technical data of a valuable importance for patients' health, specifically for the diagnosis, as well as for the treatment (namely referring to the choice of an appropriate prosthesis system, as the case). Thus, structural, chemical, and mechanical properties of several parts of the bone tissue (cartilage and bone) have been obtained through measurements performed by the two techniques. Also, discussions on their importance for medical purposes were done.

2. MATERIALS AND METHODS

2.1. MATERIALS

Bone tissue parts for the study were sampled during a surgery procedure applied on a patient suffering from severe osteoarthritis of the knee secondary to a tibial plateau malunited fracture. Patient had a *Genu varum* deformity with subchondral bone condensation. Bone pieces located on the tibial plateau, medial and lateral facets were the subject of present study.

After surgery extraction, disinfection of the bone tissue parts was performed in the medical facilities. No potential risk on the manipulating personnel could occur in the measurement actions that followed. Samples were left to dry, first at room temperature for 1 h, then for 24 h at 40 °C in a lab circulation oven.

X-ray diffraction data acquisition was performed on cartilage pieces cut with maximum dimensions of 10 x 15 mm, mounted in the aluminium sample support of the diffractometer, both with the external face, and with the internal face (in contact with the bone). Also, dried bone parts were grinded in a ceramic mortar; two fractions were separated by sieving. Data recorded on the fine fraction (max. overall size of 1 mm) are presented and discussed in the following sections. Bone samples were mounted in the standard quartz sample supports of the diffractometer.

For the nanoindentation tests, different samples (cartilage and bone) were cut from the main pieces. Small pieces for measurement had dimensions of 4 x 6 x 3 mm. No polishing or other mechanical operations were applied before measurement. For a proper fixation in the

sample tray, studied samples were mounted on a polymeric sample disk with double adhesive band, and then measured.

2.2. METHODS

X-ray Diffraction

The X-ray diffraction technique (XRD) was used to characterize the structure and chemical composition of the bone tissue samples. Data were acquired using a Rigaku Ultima IV instrument, with monochromatized Cu Kα radiation (λ = 1.54056 Å), from a fixed anode X-ray tube operated at 40 kV and 20 mA. Powder diffraction patterns were recorded for the 2-theta range of 5 – 70 degrees, in parallel beam geometry with continuous scan mode, at 1 degrees/minute speed and 0.02 degrees step width.

Whole Powder Pattern Fitting (WPPF) method was used for analysis; profile fitting was performed over a comparatively broad angular range, based on information about the crystal system and lattice constants. Data calculations were done with dedicated software PDXL v. 2.2 and ICDD data base PDF4+ v. 2015. Starred and indexed quality mark PDF cards were selected for the search – matching step.

Nanoindentation technique

Nanoindentation methods were used in the present study for the mechanical characterization of bones and cartilages, samples collected and prepared as previously described. The nanoindenting system Agilent G 200 equipped with pyramidal Berkovich indenter and Nanosuite software package were used for measurements and evaluation of microhardness and Young elasticity modulus.

Hardness and stiffness of small samples were determined by applying a contact force lower than 10 μN at a load resolution lower than 50 nN. First, the indentation procedure was performed on the glossy surface of the cartilage (*normal* indentation), along with the anatomical axis of the tibia, perpendicular to the articular surface. Then, the indentation was applied on the cartilage section (*tangential* indentation), perpendicular to the anatomical axis of the tibia, in a plane tangent to the articular surface.

3. RESULTS AND DISCUSSION

3.1. X-RAY DIFFRACTION

X-ray diffraction analysis was performed to evaluate the crystallinity of studied bone tissue, as well as to confirm presence of some crystalline phases in bone and/or cartilage samples. Thus, presence of hydroxyapatite $Ca_5(PO4)_3(OH)$, monetite $CaHPO_4$ and brushite $CaPO_3(OH)\cdot 2H_2O$ was investigated. Also, crystallite dimensions of the identified crystalline phases were determined.

Several related scientific works report correlations between presence of these phases and the bone formation process. For instance, Postic S.D. reports that changes of crystallographic structure such as transition of hydroxyapatite to monetite and brushite occur when changes in the physiologic environment appear. Also, changes in the Ca: P atomic ratios were considered subsequent to physiologic processes. Though the bone structure is considered

well defined, the subject of bone formation process is still under scientific debating. While some researchers suggest a classical nucleation and growth process, others discuss about existence of some transitory phases, either amorphous or crystalline, considered as precursors to hydroxyapatite in the bone [1, 3]. However, due to its complexity, final conclusions on processes involved in bone transformations during lifetime have not been drawn yet. Data collected through XRD may contribute to a better knowledge and evaluation of the bone changes mechanisms, especially in situations where various comparisons are possible (*i.e.* with bone tissues from the same patient sampled in a previous surgery episode on the contralateral side, or with bone pieces of other patients affected by similar pathology, etc.).

Raw data recorded from the XRD scans were inputted into PDXL software, and Rietveld analysis was performed for crystallographic refinement. Crystal models for the three substances followed were built using information from ICDD pdf cards 01-079-5683, 01-071-1759, 00-009-0077, respectively for hydroxyapatite, monetite and brushite. Details of the crystallographic models used are listed in Table 1. Peak shapes were modelled using pseudo-Voigt function, and two asymmetry parameters were refined. In each case, eight background parameters, a scale factor and three peak shape parameters were refined.

Table 1. Crystal structure parameters for hydroxyapatite, monetite and brushite

Phase (compound) name	*Chemical formula*	*Crystal system*	*Space Group*	*Density [g/cm^3]*	*ICDD - PDF card number*
Hydroxyapatite (Calcium Phosphate Hydroxide)	$Ca_5(PO4)_3(OH)$	Hexagonal	176: P63/m	3.155	01-079-5683
Monetite (Calcium Hydrogen Phosphate)	$CaHPO_4$	Triclinic	2: P-1	2.944	01-071-1759
Brushite (Calcium Phosphate Hydroxide Hydrate)	$CaPO_3(OH)\cdot 2H_2O$	Monoclinic	9: C1c1, unique-b, cell-1	2.314	00-009-0077

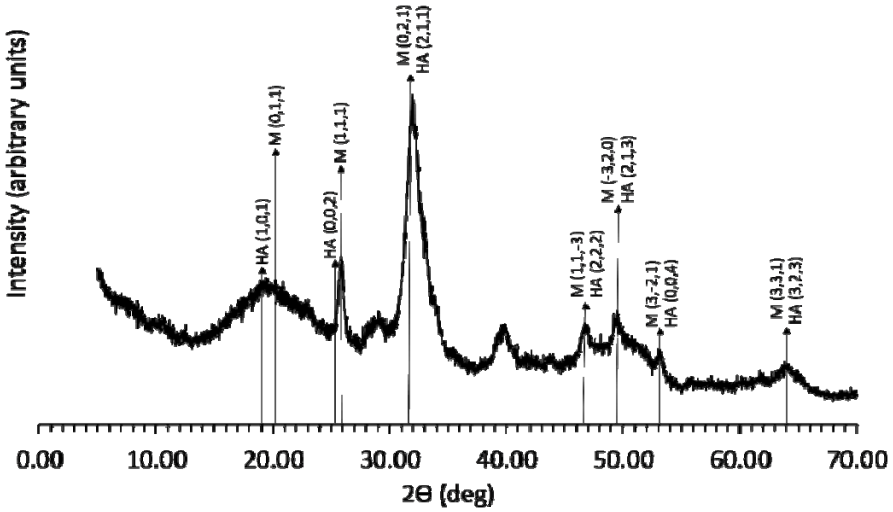

Figure 1. X-ray pattern of studied bone; HA – hydroxyapatite, M – monetite, Miller indices indicated in brackets.

Fig. 1 shows X-ray pattern recorded for the studied bone. In this figure, presence of both narrow and broad peaks may be associated with a mixed crystalline and amorphous character of the sample. Broad peaks may also be associated with presence of very low crystallite dimensions, specifically of nanometric ones [15, 16]. Also, broad, and slight asymmetric peaks may be attributed to overlapped individual peaks (from one or several compounds) obtained in the experimental conditions of X-ray pattern acquisition. Presence of nanometric sized compounds may be also associated with broad peaks in the X-ray patterns [15, 16].

Regarding the three crystalline phases searched in studied bone, hydroxyapatite (HA) and monetite (M) were confirmed to be simultaneously present in the studied sample, and recorded peaks were marked in Fig. 1 together with corresponding Miller indexes. The WPPF method indicated as quantitative results of 48 ± 2 % for HA, and 52 ± 5 % for M (phase content expressed in % w/w). Brushite phase was not found in bone sample, or its content is below detection limit of the method. Table 2 presents the comparison between experimental and standard diffraction data for the studied sample, a good agreement between these data being observed. Crystallite size was estimated from the X-ray pattern recorded for the bone sample, the Halder Wagner method has been used, results corresponding to each peak that was took into calculations are indicated in Table 2. It may be observed that nanometric dimensions have been estimated for crystallite size, values in the range 1.68 – 17. 61 nm were found.

Table 2. The values of diffraction angle and interplanar spacing of the seven fitted diffraction lines and values of crystallite size obtained from Halder – Wagner method.

Experimental data			**Standard data / ICDD cards** 01-079-5683 (HA - hydroxyapatite), 01-071-1759 (M - monetite)			
Diffraction angle - 2θ [degrees]	*Interplanar spacing - d [Å]*	*Crystallite size [Å]*	*Phase*	*Diffraction angle 2θ [degrees]*	*Interplanar spacing - d [Å]*	*Miller Indices (h, k, l)*
19.45 ± 0.16	4.56 ± 0.04	16.83 ± 0.50	HA:	18.8270	4.709500	1, 0, 1
			M:	19.8392	4.471460	0, 1, 1
25.84 ± 0.03	3.445 ± 0.004	176.11 ± 9.49	HA:	25.8740	3.440600	0, 0, 2
			M:	25.5749	3.480160	1, 1, 1
31.66 ± 0.03	2.823 ± 0.003	48.30 ± 0.93	HA:	31.7776	2.813590	2, 1, 1
			M:	31.4761	2.839850	0, 2, 1
46.59 ± 0.09	1.948 ± 0.004	68.97 ± 10.53	HA:	46.7058	1.943220	2, 2, 2
			M:	46.5341	1.949990	1, -1, 3
49.44 ± 0.17	1.842 ± 0.006	34.45 ± 4.76	HA:	49.4877	1.840300	2, 1, 3
			M:	49.2697	1.847930	-3, 2, 0
53.17 ± 0.15	1.721 ± 0.005	40.16 ± 15.46	HA:	53.2000	1.720300	0, 0, 4
			M:	53.1520	1.721740	3, -2, 1
64.13 ± 0.04	1.4509 ± 0.005	47.54 ± 2.70	HA:	64.1764	1.450010	3, 2, 3
			M:	64.0493	1.452580	3, 3, 1

The XRD study confirms presence of crystalline hydroxyapatite and monetite phases in the studied bone, while presence of crystalline brushite was not confirmed. Presence of monetite in the sample could be associated with osteoporotic disease of this patient, as this compound has a lower density (2.944 g/cm^3) than hydroxyapatite (3.155 g/cm^3). In Fig. 2, the

shape of the pattern (a) demonstrates the amorphous character of the external face of the studied cartilage. Also, shape of the pattern (b) was associated with a mixed crystalline and amorphous character of the internal face of the cartilage; the peaks (both sharp and broad) observed may be the result of a diffraction phenomenon corresponding to presence of some crystalline phases. Further investigations to identify these phases were performed; their results are indicated on the plot at corresponding diffraction angles, together with the Miller indices. Thus, it may be observed that hydroxyapatite (HA) and brushite (Br) phases are present in the sample, while the monetite phase was not found, or may be under the detection limit of the method. The RIR quantitative evaluation indicated the following phase's percentage distribution: hydroxyapatite 83 ± 19 % and brushite 17 ± 5 %. It is to be mentioned that brushite phase identified in this face of the cartilage has a density of 2.314 g/cm^3, lower than both hydroxyapatite and monetite.

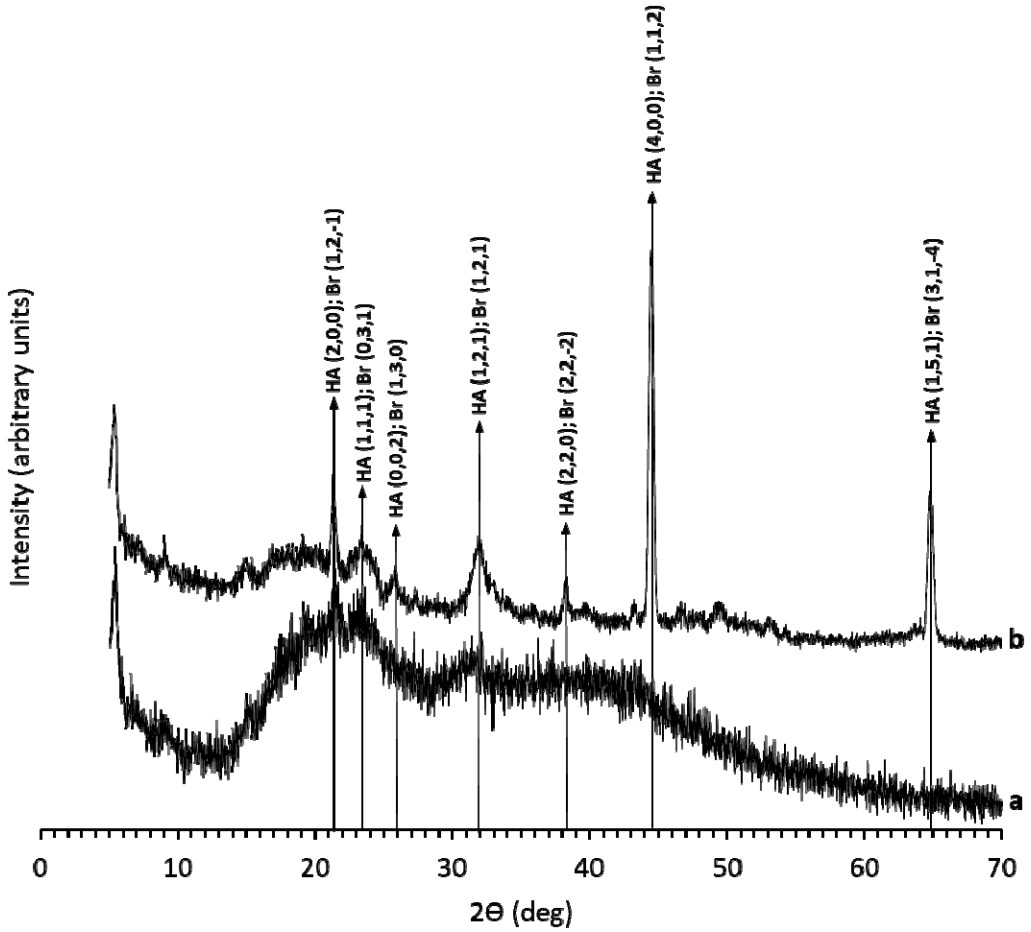

Figure 2. X-ray pattern of studied cartilage, external (a) and internal (b) faces; crystalline phase's notations: HA – hydroxyapatite, Br – brushite, Miller indices indicated in brackets.

In Fig. 2, the shape of the pattern (a) demonstrates the amorphous character of the external face of the studied cartilage. Also, shape of the pattern (b) was associated with a mixed crystalline and amorphous character of the internal face of the cartilage; the peaks (both sharp and broad) observed may be the result of a diffraction phenomenon corresponding to presence of some crystalline phases. Further investigations to identify these phases were performed; their results are indicated on the plot at corresponding diffraction angles, together with the Miller indices. Thus, it may be observed that hydroxyapatite (HA) and brushite (Br) phases are present in the sample, while the monetite phase was not found, or may be under the detection limit of the method. The RIR quantitative evaluation indicated the following phase's percentage distribution: hydroxyapatite 83 ± 19 % and brushite 17 ± 5 %. It is to be

mentioned that brushite phase identified in this face of the cartilage has a density of 2.314 g/cm^3, lower than both hydroxyapatite and monetite.

Information collected through X-ray diffraction provided information on the structural and chemical (qualitative and quantitative) characteristics of the studied bone tissue parts. To complete the overview of the patients' disease and/or its evolution, some correlations between X-ray diffraction data and other medical tests (complete blood count, bone densitometry, etc.) may be followed. In this respect, measurements at different stages of disease evolution for the same patient, both on ipsi- and contralateral side, or comparisons with other patients with similar disease could provide useful and overall information for both diagnosis and treatment.

3.2. NANOINDENTATION MEASUREMENTS

Nanoindentation was applied in several measurement setups, both on the bone parts and on the cartilage. In the following paragraphs, results obtained on cartilage only will be commented. Data acquisitions on the bone parts of the samples was found to be difficult and did not provide conclusive results; thus, as the indentation requires a smooth surface, this was impossible to reach as the sample was a bone tissue from epiphyseal area with a spongy appearance and a high roughness; various areas were addressed, on OX axis, also on OY axis, with steps of 50 µm and 100 µm, with no good results.

For the cartilage sample, the indentation procedure was first performed on its glossy surface (*normal indentation*), along with the anatomical axis of the tibia, perpendicular to the joint surface. Then, the indentation was applied on the cartilage section (*tangential indentation*), perpendicular to the anatomical axis of the tibia, in a plane tangent to the joint surface. Measurements were performed in 4 points on the cartilage surface, by applying the loading force of the instrument in 4 different points of the cartilage surfaces.

Fig. 3 shows variation of the loading force with the indentation depth, for cartilage samples indented perpendicular on the tibia axis (*tangential* indentation). Specimen 1, 2, 3 and 4 in the plot correspond to the four points on the cartilage surface where the indentation was applied.

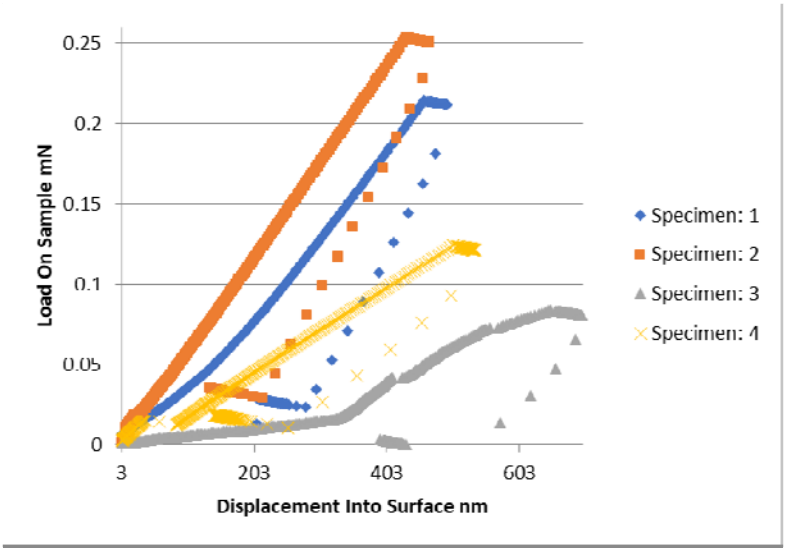

Figure 3. Variation of the loading force versus indentation depth, for cartilage tangential indentation.

Table 3 shows average values generated by Nanosuite software calculations, performed according to equations explained below.

The hardness (**H**) of the test surface is determined using the equation (1):

$$H = P/A \quad [N/m^2] \tag{1}$$

where **P** is the load applied to the test surface, and **A** is the projected contact area at that load.

The elastic modulus (**E**) of the test sample is determined from the reduced modulus, E_r, given by equation (2):

$$E_r = \frac{\sqrt{\pi} \cdot S}{2\beta\sqrt{A}} \quad [N/m^2] \tag{2}$$

where:

ß is a constant depending on the indenter geometry, here the value of 1.034 was considered, data valid for the Berkovich indenter with triangular cross-sections;

S is the slope of the upper portion of the load-displacement curve (slope of P- h curve according to Figure 4).

A has the same meaning as in equation (1), and π is the respective constant.

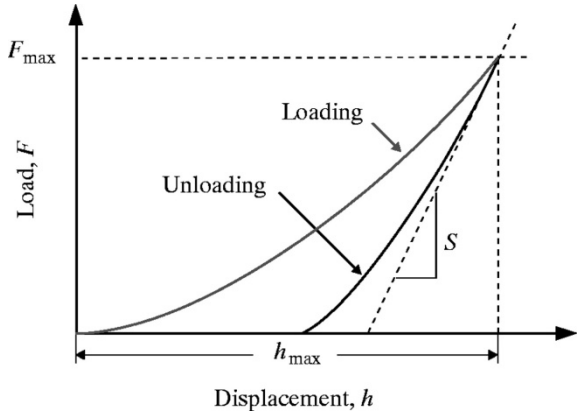

Figure 4. Load - displacement curve [17].

The elastic modulus (**E**) of the test material is calculated using the expression (3):

$$\frac{1}{E_r} = \frac{(1-\nu^2)}{E} + \frac{(1-\nu_i^2)}{E_i} \tag{3}$$

where $\boldsymbol{\nu}$ is the Poisson's ratio for the test material. $\boldsymbol{E_i}$ and $\boldsymbol{\nu_i}$ are the elastic modulus and Poisson's ratio, respectively, of the indenter.

As may be observed in Table 3, experimental findings show that *normal* indentation measurements on cartilage samples along with the anatomical axis of the tibia compared with *tangential* indentation indicate differences of one order of magnitude. Thus, while in the first setup the microhardness was of 2 MPa and Young modulus of 21 MPa, in the second setup these parameters were, respectively, of 57 MPa and 368 MPa.

Young modulus is a measure of stiffness. Its higher value suggests a higher stiffness, so a lower deformability. Experimental findings show that the cartilage has a lower hardness and a lower stiffness (more deformable) along with the anatomic axis of the tibia than perpendicular on this axis; the anisotropy is clearly observed, differences being in one order of magnitude. Considering that the cartilage was sampled from a tibial plateau with severe osteoarthritis, it was expected that it is less deformable (with a higher stiffness) and harder than a healthy cartilage [12].

Table 3. Microhardness and youg modulus for cartilage – normal and tangential indentation.

	Inputs		Outputs	
Indentation type	*Indentation depth [nm]*	*Maximum loading force [mN]*	*Microhardness [GPa]*	*Stiffness / Young Modulus [GPa]*
Tangential	530.759	0.175	0.057	0.368
Normal	14705.234	7.019	0.002	0.021

One of the main difficulties related to orthopedic implants is the weakening of the bone-cement interface, which is followed by the wear of the implant material, as well as by inflammation and necrosis of adjacent tissues. These consequences lead to the need of orthopedic implant replacement. This operation is made usually after a complete set of mechanical testing. In this respect, 3D modelling of bone parts, of the orthopedic implant and simulation of their assembly operation is particularly useful [3]. The bone mechanical properties may be summarized as follows: bone is an anisotropic material and viscoelastic (*i.e.* its mechanical properties vary with the velocity of the loading tension and very resistant [12]. Bone tissue has a specific structure, appropriate to its resistance at various mechanical stress such as pressure: functions of resistance at pressure, bending, stretching, twisting, etc. [14]. The knee is one of the most important joint in the human body, therefore, generally, researchers study actively different aspects related to its functionality. 3D modelling and operational simulation software make use of the specific material physical parameters, and therefore, their accurate measurements may be considered as a must for a successful conclusion at the patient level.

4. CONCLUSIONS

Present study proposed experimental setups for two instrumental techniques applied to investigate characteristics of human bone tissue parts. The usefulness of the two techniques has been demonstrated, information provided in this respect were related to the structure and chemical composition, and also to the microhardness and stiffness of different bone tissue parts.

The X-ray diffraction method was used to evaluate the presence of three crystalline phases (hydroxyapatite $Ca_5(PO4)_3(OH)$, monetite $CaHPO_4$ and brushite $CaPO_3(OH)\cdot 2H_2O$) in bone samples taken from a patient suffering of second degree osteoarthritis. Hydroxyapatite and monetite crystalline phases were confirmed to be present in the bone tissue Experimental data were in good correlation with standard diffraction data from ICDD PDF cards 01-079-5683 (hydroxyapatite), and 01-071-1759 (monetite). Bone samples were found to have a partial amorphous character. The X-ray recorded pattern was used for average crystallite size with Halder Wagner method. For the crystalline phases identified in studied bones, nanometric crystallite sizes in the range 1.68 – 17.61 nm were found. Quantitative analysis performed on studied bone samples showed a higher content in the lower density phase (monetite), comparing with hydroxyapatite content, this finding may be considered an indicator for the onset of an osteoporotic disease. The cartilage was proved to have an amorphous character on the external face, while a mixed crystalline and amorphous structure was found in the internal face, the one in contact with the bone. Crystalline phases of hydroxyapatite and brushite were identified in this part of the tested tissues as crystalline phases, in good correlations with PDF cards 01-079-5683, and 00-009-0077 (brushite).

The use of nanoindentation demonstrated existence of significant differences (of one order of magnitude) in the deformability of the cartilage, higher along with the tibia

anatomical axis than perpendicular on it. Thus, values of microhardness were of 2 MPa and of 57 MPa respectively, while the Young modulus measurements showed values of 21 MPa and 368 MPa respectively.

Collected information may be used in the operational simulation and compatibility of certain orthopedic implant materials with different bone tissues, with obvious benefit to patients.

REFERENCES

[1] Olsza, J.M., Cheng, X., Soo Jee, S., Kumar, R., Kim, Y.Y., Kaufman, J.M., Douglas, P. E., Gower, B. L, *Materials Science and Engineering*, **R 58**, 77, 2007.

[2] Nuss, M.R.K., von Rechenberg, B., *Open Orthop Journal*, **2**, 66, 2008.

[3] Postic, S.D., *International Journal of BioMedicine*, **4**(2), 109, 2014.

[4] Nicolescu, C.M., Olteanu, R.L., Bumbac, M., *Analytical Letters*, **50**(17), 2802, 2017.

[5] Huluba, R., Pirvu, C., Nicolescu, C., Gheorghe, M., Mindroiu, M., *Materiale Plastice*, **53**(1), 130, 2016.

[6] Calderon-Moreno, J.M., Preda, S., Predoana, L., Zaharescu, M., Anastasescu, M., Nicolescu, M., Stoica, M., Stroescu, H., Gartner, M., Mihaila, M., Serban, B.C., *Ceramic International*, **40**(1), 2209, 2014.

[7] Anastasescu, M., Teodorescu, V.S., Buiu, O., Osiceanu, P., Calderon Moreno, J.M., Predoana, L., Preda, S., Nicolescu, M., Marin, A., Serban, B.C., Stoica, M., Zaharescu, M., Gartner, M., *Ceramics International*, **40**, 11803, 2014.

[8] Stratulat, A., Serban, B.C., de Luca, A., Avramescu, V., Cobianu, C., Brezeanu, M., Buiu, O., Diamandescu, L., Feder, M., Ali, S.Z., Udrea, F., *Sensors*, **15**, 17495, 2015.

[9] Avramescu, V., de Luca, A., Brezeanu, M., Ali, S.Z., Udrea, F., Buiu, O., Cobianu, C., Serban, B.C., Gardner, J., Dumitru, V., Stratulat, A., *Proceedings of the 46th European Solid-State Device Research Conference (ESSDERC 2016)*, 280, 2016.

[10] Mihai, S., Filip, V., Vladescu M., *Journal of Science and Arts*, **2**(35), 177, 2016.

[11] Balasa, M.C., Cuculici, S., Pantu, C., Mihai, S., Negrea, A.D., Zdrafcu, M.O., Let, D.D., Filip, V., Cristea, S, *The Scientific Bulletin of Valahia University Materials and Mechanics,* **15**(13), 41, 2017.

[12] Poinescu, A.A., Radulescu, C., Vasile, B.S., Ionita, I., *Revista de Chimie*, **65**(10), 1245, 2014.

[13] Franke, O., Durst, K., Maier, V., Göken, M., Birkholz, T., Schneider, H., Hennig, F., Gelse, K., *Acta Biomaterialia*, **3**(6), 873, 2007.

[14] Nenciu, G., *Biomecanica în educaţie fizică şi sport. Aspecte generale*, Ed. Fundatiei Romania de Maine, 2005.

[15] Thakur, V.K., Carp, C.A., Pandele, A.M., Comanici, F.E., Miculescu, F., Stefan, V.I., Serban, B.C., *Vacuum*, **146**, 599, 2017.

[16] de Luca, A., Udrea, F., Li, G., Zeng, Y., André, N., Pollissard-Quatremère, G., Francis, L.A., Flandre, D., Racz, Z., Gardner, J.W., Ali, S.Z., Buiu, O., Serban, B.C., Cobianu, C., Wotherspoon, T., *Sensors and Sensor Systems for Harsh Environment Applications*. Book chapter in *Semiconductor Devices in Harsh Condition*, CRC Press, Taylor & Francis Group, 2016.

[17] Barbakadze, N., Enders, S., Gorb, S., Arzt, E., *Journal of Experimental Biology*, **209**, 722, 2006.